JOURNAL OF THEORETICAL
AND APPLIED MECHANICS
51, 2, pp. 393-407, Warsaw 2013

CLOSED-FORM SOLUTIONS FOR TORSION ANALYSIS OF STRUCTURAL BEAMS CONSIDERING WEB-FLANGE JUNCTIONS FILLETS

S-Zahra Shahpari, Mohammad R. Hematiyan
Shiraz University, Department of Mechanical Engineering, Shiraz, Iran
e-mail: zahra.shahpari@gmail.com; mhemat@shirazu.ac.ir

In this paper, an effective semi-analytical method is presented for torsion analysis of structural beams with various kinds of junctions such as T, I, H, E and + beams. A fairly simple but precise formulation based on analytical and accurate numerical solutions is presented for evaluating the shearing stress at critical points and computing the torsional rigidity of a member under torsion. The problem is formulated based on Prandtl's stress function. The cross-section is decomposed into several segments, including straight, curved, end, and junction segments. The torsion problem is solved in each segment separately. Standard junction segments are analyzed using the finite element method with a fine mesh. Other segments are analyzed by analytical methods. Closed-form expressions in terms of geometrical parameters are found for the shearing stresses at critical points of each segment. The torsional rigidity of the cross section is also expressed by a closed-form expression. The presented formulations can be used for analysis of a wide range of thin- to moderately thick-walled complicated sections.

Key words: torsion, shearing stress, torsional rigidity, fillet

1. Introduction

In early studies on the torsion problem, simple or thin-walled cross-sections have been considered. According to the thin-walled theory, the shearing stress and torsional rigidity of a simple open cross-section can be estimated by analyzing a thin rectangle (Sadd, 2009). There exists an exact solution for a rectangular member under torsion (Pagano and Chou, 1992; Sadd, 2009). Although the formulation based on the thin-walled theory is relatively simple, but it cannot predict acceptable values for the shearing stress at corners (Pagano and Chou, 1992; Timoshenko and Goodier, 1970).

El Darwish and Johnston (1965) presented a method for approximate torsion analysis of some structural shapes such as T-beams. They used the finite difference method to solve the torsion Poisson equation in terms of Prandtl's stress function. They presented a formulation for the evaluation of the torsional rigidity and shearing stress at the midpoint of the flange of the T-beam. However, evaluation of the shearing stress at the web-flange junction fillet of the T-beam is impossible by the method presented by El Darwish and Johnston.

Chen and Chen (1981) proposed an analytical solution based on the Laplace equation for torsion analysis of beams with +, I, [, T and some other similar cross-sections. They divided the cross-section of the beam into some rectangular sub-domains. In their method, the unknown displacements on the boundaries of these sub-domains are found by solving a system of equations. They presented some formulas for torsion of these beams; however, corner fillets were ignored in their formulation.

Lee *et al.* (2007) studied behavior of a composite double T-section beam under torsional loading using the finite element method (FEM). They obtained stiffness matrix elements by minimization of the total potential energy.

Hematiyan and Doostfatemeh (2007) proposed an analytical approximate method for analyzing the torsion problem of a hollow isotropic polygonal shape. This method is capable of predicting the variation of the shearing stress across the thickness of the beam. Moreover, this method results in acceptable solutions for thin-walled to moderately thick-walled beams; however, the method cannot be used for open section members.

Doostfatemeh *et al.* (2009) presented some analytical formulas for torsion analysis of beams, including straight and curved segments with different thicknesses. Their formulation can be used for hollow members, but it cannot be employed for torsion analysis of open section members such as T-beams. Arghavan and Hematiyan (2009) extended the method presented by Doostfatemeh *et al.* (2009) to analyze non-homogenous hallow members under torsion.

Hematiyan and Estakhrian (2011) presented an approximate analytical method for torsion analysis of members with open cross-sections containing straight and curved segments with a uniform thickness. They solved Poisson's equation in each segment separately, and obtained closed-form formulas for the shearing stress and torsional rigidity of the member. This is a simple and accurate method for torsion analysis of thin-walled as well as moderately thick-walled sections; however, it cannot be used for torsion analysis of members with a junction, such as a T-beam.

The torsion problem of members with three- and four-way segments, such as T, I and + beams have been studied rarely. The thin-walled theory could not predict an accurate value for the angle of twist of these members. Moreover, it is impossible to evaluate the value of the shearing stress at fillets using the thin-walled theory.

The objective of this paper is to present a formulation for torsion analysis of open-section members with three- and/or four-way segments. Closed-form expressions in terms of geometrical parameters are found for the evaluation of torsional rigidity and shearing stresses at critical points of the member. The presented formulations are practical and can be used for analysis of a wide range of thin- to moderately thick-walled complicated sections. Beams with three- or four-way segments are widely used in various industries such as aeronautics, aerospace, and marine. These beams may be subjected to a combination of torsion and other loadings such as bending moment, shear, and axial forces. This paper is focused on the torsion analysis. If the beam is subjected to a compound loading, the total stresses can be easily found using a simple superposition technique.

2. Governing equations

Consider a uniform member with an arbitrary open cross-section, including three-way and/or four-way segments as shown in Fig. 1. The member is subjected to two equal torques with opposite directions at two its ends. The z-direction coincides with the longitudinal axis, and the cross-section is in the xy plane.

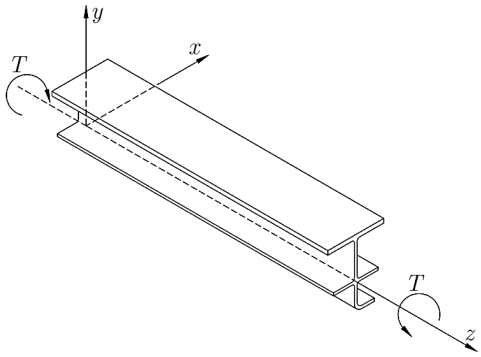

Fig. 1. Torsion of a general open-section beam consisting of three- and four-way segments

Boundary conditions and governing equations of the torsion problem can be efficiently expressed in terms of Prandtl's stress function (Sadd, 2009). The shearing stresses in the cross-section can be expressed as follows:

$$\tau_{xz} = \frac{\partial \phi}{\partial y} \qquad \tau_{yz} = -\frac{\partial \phi}{\partial x} \tag{2.1}$$

where τ_{xz} and τ_{yz} are the shearing stresses in the x- and y-direction, respectively, and ϕ is Prandtl's stress function. The governing equation for Prandtl's stress function can be expressed as

$$\nabla^2 \phi = -2G\alpha \tag{2.2}$$

where G is the shear modulus of elasticity, and α is the angle of twist per unit length. Equations (2.1) and (2.2) satisfy equilibrium and compatibility equations. Since the considered cross-section is a simply connected domain, the boundary condition on boundaries of the cross-section can be expressed as $\phi = 0$. The applied torque can be expressed in terms of ϕ as follows

$$T = 2 \iint \phi \, dx \, dy \tag{2.3}$$

The torsion problem can also be expressed in a dimensionless form, see for example Gorzelańczyk (2011). The dimensionless relationships can be derived by defining the following dimensionless parameters

$$\begin{aligned} x^* &= \frac{x}{t_f} \qquad & y^* &= \frac{y}{t_f} \qquad & t_w^* &= \frac{t_w}{t_f} \qquad & r^* &= \frac{r}{t_f} \\ \phi^* &= \frac{\phi}{G\alpha t_f^2} \qquad & \tau^* &= \frac{\tau}{G\alpha t_f} \qquad & T^* &= \frac{T}{G\alpha t_f^4} \end{aligned} \tag{2.4}$$

where x^* and y^* are dimensionless coordinates, ϕ^* is dimensionless Prandtl's stress function, τ^* is the dimensionless shearing stress, and T^* is the dimensionless torque. t_f is a characteristic length denoting the thickness of the flange. Substituting the parameters given in Eq. (2.4) into Eqs (2.1), (2.2), and (2.3) the following relationships are found

$$\tau_{xz}^* = \frac{\partial \phi^*}{\partial y^*} \qquad \tau_{yz}^* = -\frac{\partial \phi^*}{\partial x^*} \qquad \frac{\partial^2 \phi^*}{\partial x^{*2}} + \frac{\partial^2 \phi^*}{\partial y^{*2}} = -2 \qquad T^* = 2 \iint \phi \, dx \, dy \tag{2.5}$$

The boundary condition on boundaries of the cross-section can be expressed as $\phi^* = 0$.

3. Problem modeling and formulation

An open cross-section containing a three-way and a four-way segment is shown in Fig. 2. The section shown in Fig. 2 is not a standard section, but it can be considered as a general section that most of practical members such as I-, T- and L- beams may be extracted from. Contour lines of constant ϕ are also shown in Fig. 2. To solve the torsion problem over a cross-section, like the one shown in Fig. 2, the cross-section is decomposed into several straight, curved, and end segments. A three-way and a four-way segment as shown in Fig. 2, should also be considered. Through appropriate approximations, the torsion problem is solved over each segment separately. The methods for analyzing the problem in straight, curved, and end segments are completely presented in (Hematiyan and Estakhrian, 2011). The focus of this work is to analyze the three- and four-way segments. Contour lines in straight and curved segments are assumed parallel to external boundaries (Hematiyan and Estakhrian, 2011). The solution in end segments can be found using the relationships for rectangular members (Hematiyan and Estakhrian, 2011). However, the problem is more complicated in the three- and four-way segments. In the following sections, the methods for modeling and formulating the problem in straight, curved, and end segments are reviewed, and the method for solving the problem in junction segments is presented.

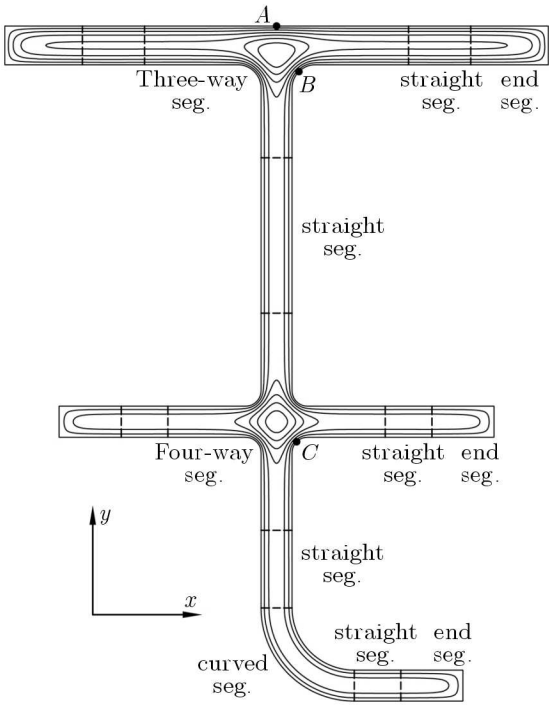

Fig. 2. Contour lines in an open cross-section, containing three- and four-way segments

3.1. Formulation for straight segments

In straight segments, the contour lines are assumed parallel to the boundary, as shown in Fig. 3.

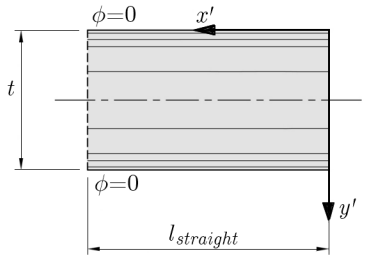

Fig. 3. Contour lines in a straight segment

The relationship for the shearing stress in a straight segment can be expressed as follows (Hematiyan and Estakhrian, 2011)

$$\tau = \left|\frac{d\phi}{dy'}\right| = G\alpha|t - 2y'| \tag{3.1}$$

where y' is the thickness coordinate as shown in Fig. 3. The relationship for the torque corresponding to a straight segment with the length $l_{straight}$ and thickness t is (Hematiyan and Estakhrian, 2011)

$$\frac{T_{straight}}{\alpha} = G\frac{l_{straight}t^3}{3} \tag{3.2}$$

3.2. Formulation for curved segments

A curved segment with the angle β, internal and external radii r_1 and r_2, and the polar coordinate system (r, θ) is shown in Fig. 4. The contour lines are assumed parallel to the boundary (Hematiyan and Estakhrian, 2011), as shown in Fig. 4.

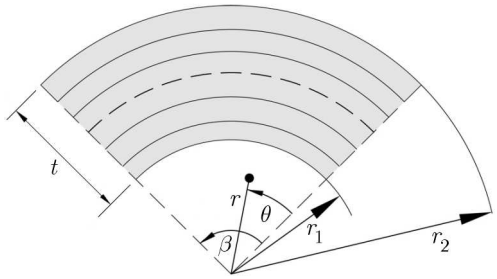

Fig. 4. The geometry and contour lines of a curved segment

The relationships for the shearing stress in the inner and outer radius of a curved segment can be expressed as follows (Hematiyan and Estakhrian, 2011)

$$\tau_{inner} = \frac{G\alpha t\overline{R}}{r_1 \ln(r_2/r_1)} - G\alpha r_1 \qquad \tau_{outer} = G\alpha r_2 - \frac{G\alpha t\overline{R}}{r_1 \ln(r_2/r_1)} \tag{3.3}$$

where t and $\overline{R}$ are the thickness and mean radius, respectively. The torsional rigidity corresponding to the curved segment can be expressed as follows (Hematiyan and Estakhrian, 2011)

$$\frac{T_{curve}}{\alpha} = \beta G\overline{R}t\Big[\frac{1}{2}(r_1^2 + r_2^2) - \frac{\overline{R}t}{\ln(r_2/r_1)}\Big] \tag{3.4}$$

3.3. Formulation for end segments

An end segment is shown in Fig. 5. Dimensions of the end segment are $t \times 2t$. This segment can be modeled with a very good approximation as one-half of a $t \times 4t$ rectangle under torsion. Using the exact solutions for a rectangle under torsion, the relationship for torque corresponding to the end segment can be found as follows (Hematiyan and Estakhrian, 2011)

$$\frac{T_{end}}{\alpha} = 0.5620Gt^4 \tag{3.5}$$

The maximum shearing stress in the end segment is (Hematiyan and Estakhrian, 2011)

$$\tau_{max} = 0.9970G\alpha t \tag{3.6}$$

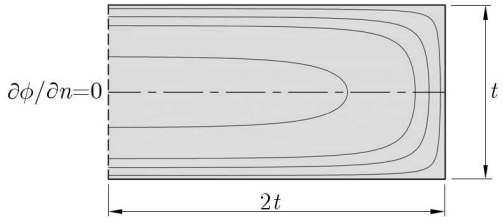

Fig. 5. Contour lines in the end segment

3.4. Formulation for three-way segments

A three-way segment with contour lines is shown in Fig. 6. The flange thickness, web thickness and fillet radius are represented by t_f, t_w, and r, respectively. The dimensions and the critical points A and B are shown in the figure. It is assumed that this segment is connected to other three segments. In standard hot-rolled sections, t_f is always greater than t_w and less than $2t_w$ (British Standard, 1993). In this work, we have assumed $1/3 \leqslant t_w^* \leqslant 1$, which is a range wider than that in the standard sections. The wide range $0.05 \leqslant r^* \leqslant 2t_w^*$ is considered for the fillet radius.

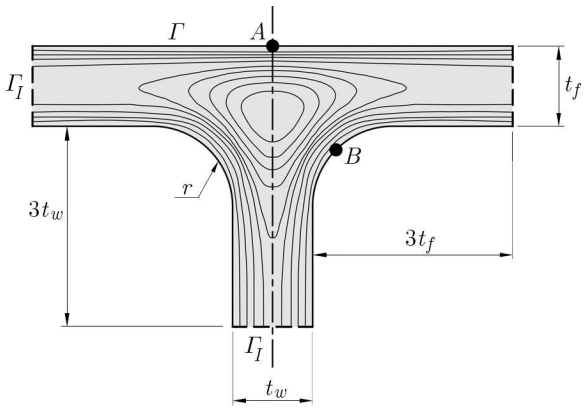

Fig. 6. Geometry and contour lines in the three-way segment

The main boundary of the segments is denoted by Γ, while the interface boundaries are represented by Γ_I. It is also assumed that the contour lines are perpendicular to the interface boundaries Γ_I. By numerical experiments using the FEM, it can be shown that this assumption is valid with a very good accuracy. The boundary conditions for the three-way segment, in a dimensionless form, can be expressed as follows

$$\phi^* = 0 \quad \text{on} \quad \Gamma \qquad \text{and} \qquad \frac{\partial \phi^*}{\partial n^*} = 0 \quad \text{on} \quad \Gamma_I \tag{3.7}$$

where n^* represents the dimensionless coordinate in the direction perpendicular to Γ_I.

We want to find a closed-form relationship for expressing the torque in terms of geometrical dimensions. Two formulas for the shearing stresses at the critical points A and B should be found too. For this purpose, many reference cases with different geometrical dimensions are considered, and the torsion problem is analyzed in each case using the FEM with a fine mesh. A developed MATLAB code based on the method described in the book by Reddy (1993) has been used for the finite element analysis. Quadrilateral 8-node quadratic elements are used in the FEM. Because of the symmetry, only one-half of the segment area is modeled in the finite element analysis. After solving the reference problems, the closed-form relationships for the torque and shearing stresses are found by an appropriate curve fitting. The employed curve fitting method is described in Appendix A.

3.4.1. Relationship for shearing stress at point A

The maximum shearing stress on the top edge of the three-way segment occurs at the point A (Fig. 6). The results for variation of the shearing stress at the point A with respect to the dimensionless web thickness ($t_w^* = t_w/t_f$) and dimensionless fillet radius ($r^* = r/t_f$) are demonstrated in Fig. 7. These results have been obtained by solving a large number of problems using the FEM with a fine mesh. As it can be seen, for a fixed flange thickness, increasing the web thickness or increasing the fillet radius results in an increase in the shearing stress.

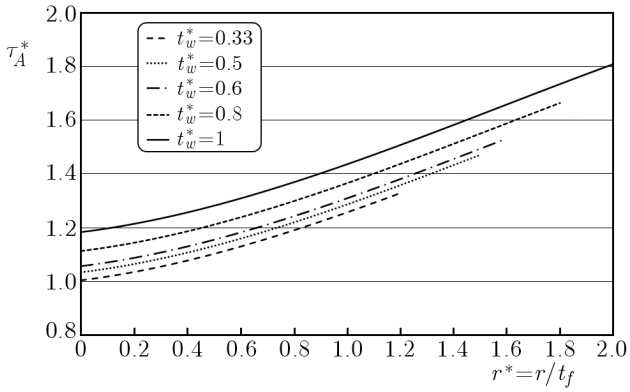

Fig. 7. Variation of the dimensionless shearing stress at the point A on the three-way segment versus the dimensionless fillet radius for different thickness ratios

To find a closed-form relationship for the shearing stress at the point A, the following six-constant function is considered

$$\tau_A^* = \frac{\tau_A}{G\alpha t_f} = A_1 + A_2 t_w^* + A_3 {t_w^*}^2 + A_4 r^* + A_5 {r^*}^2 + A_6 {r^*}^3 \tag{3.8}$$

After curve fitting, the following values for constants are obtained

$$\begin{aligned} &A_1 = 0.9704 \qquad A_2 = 0.037997 \qquad A_3 = 0.1742 \\ &A_4 = 0.1232 \qquad A_5 = 0.1640 \qquad A_6 = -0.03469 \end{aligned} \tag{3.9}$$

The maximum error in the results obtained from Eq. (3.8) in comparison with the original FEM results is only 1.4%. The R^2 value for the curve fit is 0.9988, which shows a very good agreement of Eq. (3.8) to the FEM results.

3.4.2. Relationship for shearing stress at point B

Similar FEM results were obtained for the shearing stress at the point B. Figure 8 demonstrates variation of the dimensionless shearing stress with respect to the dimensionless fillet radius for different thickness ratios. As it can be seen, the shearing stress has a downward-upward trend. Because of the presence of stress concentration at the fillet, the shearing stress goes to infinity when the fillet radius approaches to zero. This means there should be a singularity at $r^* = 0$ in the relationship expressing the shearing stress.

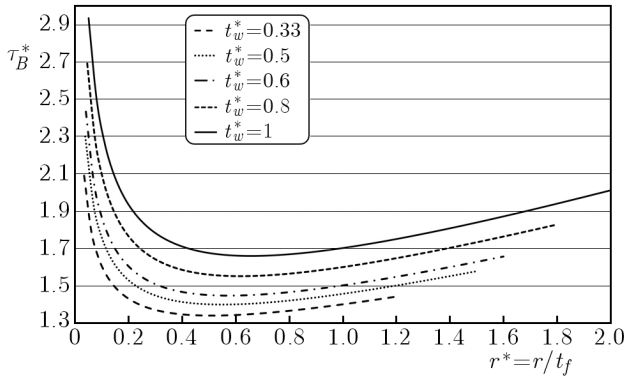

Fig. 8. Variation of the dimensionless shear stress at the point B on the three-way segment versus the dimensionless fillet radius for different thickness ratios

To find a relationship for the shearing stress at the point B, a function including three constants with a singular term is considered. The power of the singular term is selected by a

trial and error process in the curve fitting procedure. The function with the three constants is as follows

$$\tau_B^* \equiv \frac{\tau_B}{G\alpha t_f} = A' + B' r^* + C' \frac{1}{\sqrt{r^*}} \tag{3.10}$$

The computed values for the constants appearing in Eq. (3.10) for different thickness ratios are given in Table 1. The maximum error of this formula is 1.33%, and the R^2 value is 0.9994.

Table 1. Numerical values of coefficients in Eq. (3.10)

t_w^*	A'	B'	C'
1	0.7752	0.4480	0.4801
0.9	0.7820	0.4301	0.4379
0.8	0.7887	0.4123	0.3958
0.7	0.7980	0.3940	0.3586
0.6	0.8103	0.3687	0.3242
0.5	0.8278	0.3488	0.2838
0.4	0.8541	0.3159	0.2483
0.33	0.8804	0.3029	0.2130

Table 1 represents the values of coefficients appearing in Eq. (3.10) for different thickness ratios. These coefficients can also be expressed by mathematical expressions. After curve fitting, the following relationships are obtained

$$\begin{aligned} &A' = 0.05257\frac{1}{t_w^*} + 0.7226 \qquad\qquad B' = 0.0985 + 0.35058\sqrt{t_w^*} \\ &C' = 0.08739 + 0.3903 t_w^* \end{aligned} \tag{3.11}$$

By combining Eqs. (3.10) and (3.11), the following relationship is obtained

$$\frac{\tau_B}{G\alpha t_f} = 0.05257\frac{1}{t_w^*} + 0.7226 + (0.0985 + 0.35058\sqrt{t_w^*})r^* + (0.08739 + 0.3903 t_w^*)\frac{1}{\sqrt{r^*}} \tag{3.12}$$

The shearing stresses computed using Eq. (3.12) has an error less than 1.6%.

3.4.3. Relationship for torque corresponding to three-way segment

Accurate finite element results for the dimensionless torque with respect to the dimensionless fillet radius for the three-way segment are shown in Fig. 9. The dimensionless torque rises with the increase of the dimensionless fillet radius. Furthermore, it can be seen that the dimensionless torque rises with the increasing thickness ratio t_w^*.

According to the results shown in Fig. 9, a quadratic function is considered for expressing the torque. The dimensionless torque for the three-way segment can be expressed as follows

$$T_{three-way}^* \equiv \frac{T_{three-way}}{G\alpha t_f^4} = A_T r^{*2} + B_T r^* + C_T \tag{3.13}$$

The coefficients in Eq. (3.13) are found using the curve fitting procedure for different values of t_w^*. Appropriate relationships in terms of t_w^* have also been found for expressing the coefficients in Eq. (3.13). The final relationship for torque can be expressed as follows

$$\begin{aligned} \frac{T_{three-way}}{G\alpha t_f^4} &= 1.175 {t_w^*}^{0.670} r^{*2} + \left(0.03459\frac{1}{t_w^*} - 0.08582\right) r^* \\ &+ \left(2.299 - 3.445\sqrt{{t_w^*}^3} + 4.794 {t_w^*}^2\right) \end{aligned} \tag{3.14}$$

The maximum error of Eq. (3.14) is less than 1.7%, and the R^2 value is 0.9996.

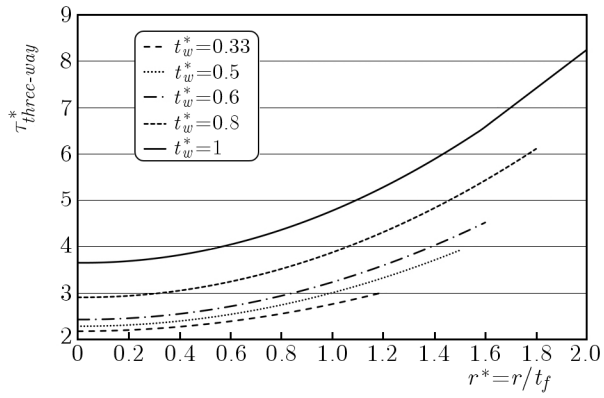

Fig. 9. Variation of the dimensionless torque versus the dimensionless fillet radius for different thickness ratios of the three-way segment

3.5. Formulation for four-way segments

A four-way segment with contour lines is shown in Fig. 10. The thicknesses are indicated by t_f and t_w. The fillet radius is denoted by r. Other dimensions and the critical point C are shown in the figure. The boundary conditions for this for-way segment can be expressed as follows

$$\phi^* = 0 \quad \text{on} \quad \Gamma \qquad \text{and} \qquad \frac{\partial \phi^*}{\partial n^*} = 0 \quad \text{on} \quad \Gamma_I \tag{3.15}$$

where Γ represents the traction free boundaries, and Γ_I represents the four interface lines of the segment. n^* represents the dimensionless coordinate in the direction perpendicular to Γ_I. The formulation is obtained for $1/3 \leqslant t^*_w \leqslant 1$, and $0.05 \leqslant r^* \leqslant 2t^*_w$.

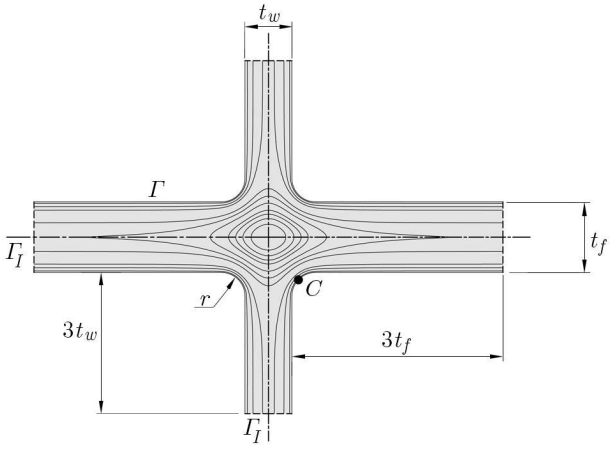

Fig. 10. Geometry and contour lines in the four-way segment

The same approach as the one used for three-way segments is used for the four-way segments. The final form of the derived formulas for the shearing stress at the point C and the torque can be expressed as follows

$$\begin{aligned}
&\frac{\tau_C}{G\alpha t_f} = 0.01434\frac{1}{t^*_w} + 0.8427 + (0.4074 + 0.2588t^*_w)r^* + (0.05947 + 0.4602t^*_w)\frac{1}{\sqrt{r^*}} \\
&\frac{T_{four-way}}{G\alpha t_f^4} = 4.156 - 4.358\sqrt{t^*_w} + 5.216{t^*_w}^2 + \left(0.3736 + 1.693\sqrt{{t^*_w}^3}\right)\sqrt{{r^*}^3} \\
&\quad + (0.4994 + 0.4801t^*_w){r^*}^3
\end{aligned} \tag{3.16}$$

The maximum error of Eq. $(3.16)_1$ is 2.2% and the R^2 value is 0.9987. The maximum error of Eq. $(3.16)_2$ is 1.8% and the R^2 value is 0.9999.

4. Formulation for torsional analysis of some structural beams

In this Section, closed-form formulas for the torsional rigidity and the shearing stresses at critical points of two important structural beams are presented.

4.1. T-beams

Consider a T cross-section as demonstrated in Fig. 11. This section includes three straight segments, three end segments, and a three-way junction segment. Using the torque formulas given in Eqs. (3.2), (3.5) and (3.14) for the straight, end and three-way segments, the closed form torque formula for the whole T cross-section can be found. This formula can be expressed as follows

$$\begin{aligned}\frac{T}{G\alpha} &= \frac{(d-5t_w-t_f)t_w^3}{3}+\frac{(b-10t_f-t_w)t_f^3}{3}+0.5620t_w^4+1.1240t_f^4\\ &+t_f^4\Big\{1.175\Big(\frac{t_w}{t_f}\Big)^{0.670}\Big(\frac{r}{t_f}\Big)^2+\Big(0.03459\frac{t_f}{t_w}-0.08582\Big)\frac{r}{t_f}\\ &+\Big[2.299-3.445\sqrt{\Big(\frac{t_w}{t_f}\Big)^3}+4.794\Big(\frac{t_w}{t_f}\Big)^2\Big]\Big\}\\ b\geqslant t_w+10t_f &\qquad d\geqslant t_f+5t_w\end{aligned} \tag{4.1}$$

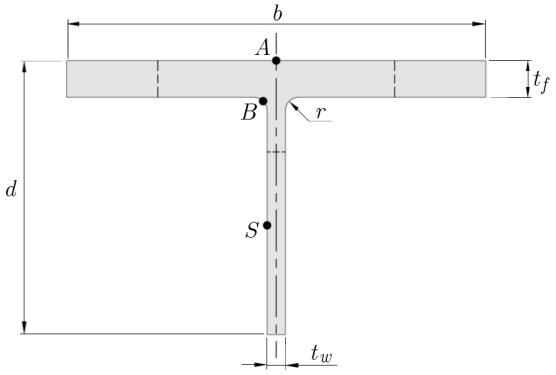

Fig. 11. T cross-section

The shearing stresses at the points A and B can be expressed as follows

$$\begin{aligned}\tau_A &= G\alpha t_f\Big[0.9704+0.037997\frac{t_w}{t_f}+0.1742\Big(\frac{t_w}{t_f}\Big)^2+0.1232\frac{r}{t_f}+0.1640\Big(\frac{r}{t_f}\Big)^2\\ &-0.03469\Big(\frac{r}{t_f}\Big)^3\Big]\\ \tau_B &= G\alpha t_f\Big\{0.05257\frac{t_f}{t_w}+0.7226+\Big(0.0985+0.35058\sqrt{\frac{t_w}{t_f}}\Big)\frac{r}{t_f}\\ &+\Big(0.08739+0.3903\frac{t_w}{t_f}\Big)\sqrt{\frac{t_f}{r}}\Big\}\end{aligned} \tag{4.2}$$

The shearing stress at the point S on the straight segment can found using the expression $\tau_S = G\alpha t_w$.

4.2. Formulation for + beams

Consider a + cross-section as shown in Fig. 12. Having the torsional rigidity formulas given in Eqs (3.2), (3.5) and $(3.16)_2$ for straight, end, and four-way segments, the closed-form torque formula for the whole + cross-section can be expressed as follows

$$\begin{aligned}\frac{T}{G\alpha} &= \frac{(f-10t_w-t_f)t_w^3}{3}+\frac{(e-10t_f-t_w)t_f^3}{3}+1.1240(t_w^4+t_f^4)\\ &+t_f^4\Big\{4.156-4.358\sqrt{\frac{t_w}{t_f}}+5.216\Big(\frac{t_w}{t_f}\Big)^2+\Big[0.3736+1.693\sqrt{\Big(\frac{t_w}{t_f}\Big)^3}\Big]\sqrt{\Big(\frac{r}{t_f}\Big)^3}\\ &+\Big(0.4994+0.4801\frac{t_w}{t_f}\Big)\Big(\frac{r}{t_f}\Big)^3\Big\}\\ e\geqslant t_w+10t_f &\qquad f\geqslant t_f+10t_w\end{aligned} \tag{4.3}$$

The shearing stress at the fillet point C can be computed from Eq. $(3.16)_1$, which yields to

$$\tau_C = G\alpha t_f\Big[0.01434\frac{t_f}{t_w}+0.8427+\Big(0.4074+0.2588\frac{t_w}{t_f}\Big)\frac{r}{t_f}+\Big(0.05947+0.4602\frac{t_w}{t_f}\Big)\sqrt{\frac{t_f}{r}}\Big] \tag{4.4}$$

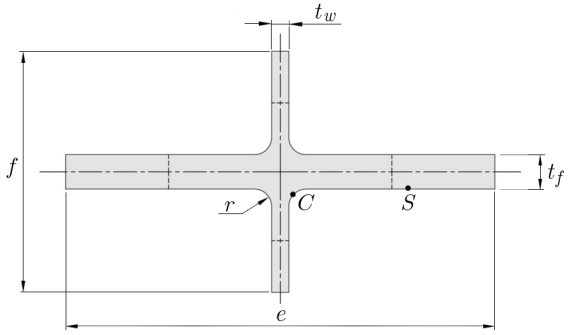

Fig. 12. + cross-section

5. Numerical study

In this Section, a numerical example for torsion analysis of T beams is presented. The results obtained by the proposed method are compared with those obtained from the FEM with a fine mesh. In some cases, the results are also compared with those obtained using the method presented by El Darwish and Johnston (1965). In the example, it is assumed that $G = 70\,\text{GPa}$ and $\alpha = 0.1\,\text{rad/m}$. A beam with the T cross-section similar to the one shown in Fig. 11 with $d = 0.4\,\text{m}$ and $b = 0.44\,\text{m}$ is considered. The torsion analyses have been carried out for different values of the thickness and fillet radius.

Figure 13 shows the shearing stresses at the two critical points A and B with $t_f = t_w = 0.02\,\text{m}$ for different values of the fillet radius. The results obtained by the present method are compared with the FEM solutions. The thin-walled theory solution and the results for the shearing stress at the point A obtained by El Darwish and Johnston method (1965) are also presented in Fig. 13. The method presented by El Darwish cannot predict the shearing stress at the point B. Figure 13 shows that the results obtained by the presented formulas are in excellent agreement with the FEM results. It can also be seen that the results obtained by the thin-walled theory for the shearing stress are considerably less than values of the shearing stresses at the points A and B. Variation of the torque with respect to the fillet radius is illustrated in

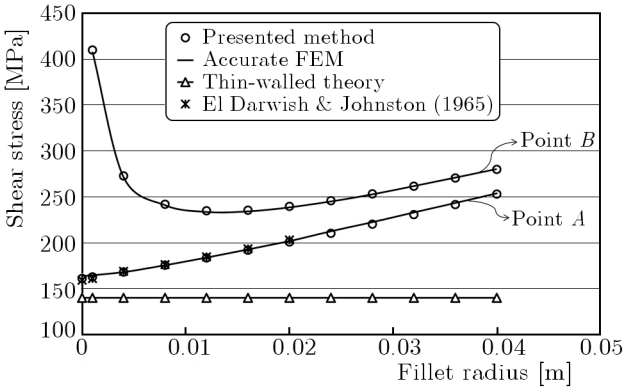

Fig. 13. Variation of the shearing stresses in the T-beam with respect to the fillet radius

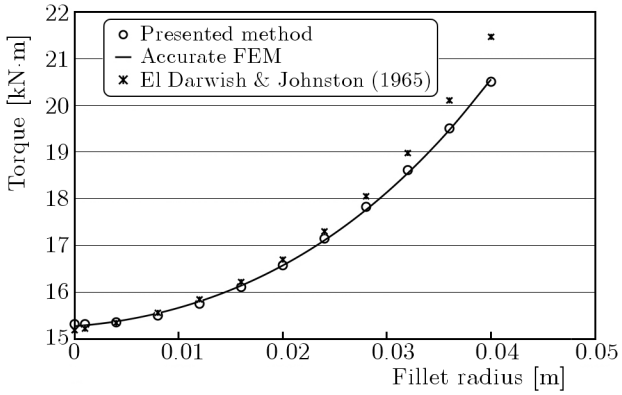

Fig. 14. Variation of the torque in the T-beam with respect to the fillet radius

Fig. 14. The obtained results are compared with the FEM solution and the results based on the El Darwish and Johnston method.

Figure 15 shows the shearing stresses at the two critical points A and B with $r = 0.008\,\mathrm{m}$ for different values of the thickness ($t_f = t_w$). The results obtained by the present method are compared with the FEM solutions. The results obtained using the thin-walled theory and the El Darwish and Johnston method are shown in this figure. The results for the torque with respect to the thickness in comparison with the FEM solution and the results obtained by the El Darwish and Johnston method are shown in Fig. 16. As it can be seen from Figs. 15 and 16, the results obtained by the present method are in excellent agreement with the accurate FEM solutions.

6. Conclusion

A method for torsion analysis of structural members, including three- or four-way junctions was presented. By the presented method, closed-form formulas can be derived for the evaluation of the torsional rigidity and the shearing stresses in a beam containing corner fillets. With these closed-form formulas, one can simply analyze, design, or optimize a structural member under torsion. For example, for a T-beam under torsion, it was shown that there is an optimum value for the corner radius to minimize the maximum shearing stress. By presenting numerical examples, it was seen that the accuracy of the proposed method is excellent. However, the thin-walled theory cannot estimate an acceptable value for the shearing stress at the corner points even for thin-walled members. The method presented in this paper can be used efficiently for thin- to moderately thick-wall members. In this paper, the focus was on the torsion analysis. When a

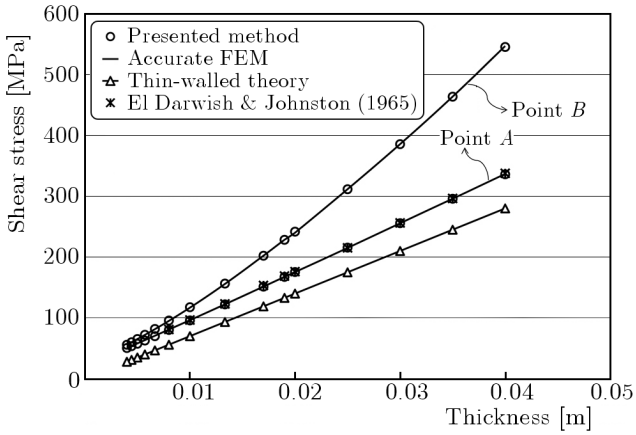

Fig. 15. Variation of the shearing stresses in the T-beam with respect to thickness

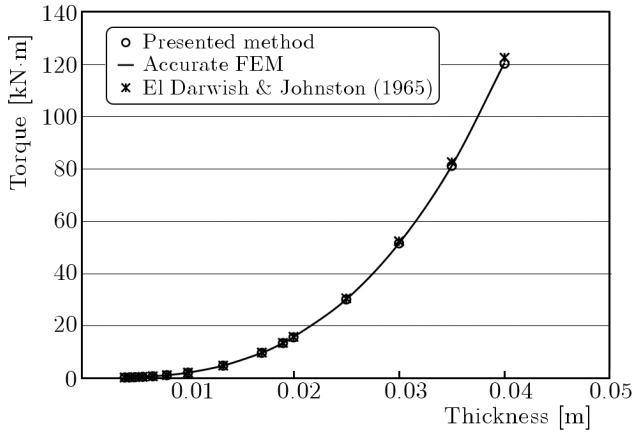

Fig. 16. Variation of the torque in the T-beam with respect to thickness

beam is subjected to a combination of various loads such as torsion, bending moment, shear, and axial forces, the total deformations and stresses can be found using a superposition technique.

A. Appendix – the curve fitting method

The method for curve fitting used in this paper is based on the least square method. This method is described briefly in this Section. A simple set, including n points (x_i, y_i), $i = 1, 2, 3, \ldots, n$, where x_i is the independent variable and y_i is the dependent variable, is considered. The function $y = f(x; c_1, c_2, \ldots, c_m)$ is going to fit on these data. c_1 to c_m in this function are unknown constants, which should be determined in a way that the summation of the squares of errors between the original and fitted values is minimum. This summation can be expressed as follows

$$S_{err} = \sum_{i=1}^{n} [y_i - f(x_i, c_1, c_2, \ldots, c_m)]^2 \tag{A.1}$$

The minimum of the above summation can be found by setting its gradient equal to zero

$$\frac{\partial S_{err}}{\partial c_j} = 0 \qquad j = 1, 2, 3, \ldots, m \tag{A.2}$$

Therefore, m equations are generated, which should be solved simultaneously. Solving this system of equations gives m constants appearing in the function f. In order to analyze the accuracy

of the fitted curve, the coefficient of determination (R^2) is evaluated. The coefficient of determination can be found as follows

$$R^2 = 1 - \frac{S_{err}}{S_{tot}} \tag{A.3}$$

where

$$S_{err} = \sum_i [y_i - f(x_i)]^2 \qquad S_{tot} = \sum_i (y_i - \overline{y})^2 \qquad \overline{y} = \frac{1}{n}\sum_{i=1}^{n} y_i \tag{A.4}$$

R^2 values near unity indicate a close relationship between the fitted function and original data.

References

1. Arghavan S., Hematiyan M.R., 2009, Torsion of functionally graded hollow tubes, *Europ. J. Mech. A/Solids*, **28**, 3, 551-559

2. British standards Institution, 1993, *British Standard*, Specification for hot-rolled sections, BS 4: Part 1

3. Chen Y.Z., Chen Y.H., 1981, Solutions of the torsion problem for bars with -, [-, +-, and T cross-section by a harmonic function continuation technique, *International Journal of Engineering Science*, **19**, 6, 791-804

4. Doostfatemeh A., Hematiyan M.R., Arghavan S., 2009, Closed-form approximate formulas for torsional analysis of hollow tubes with straight and circular edges, *Journal of Mechanics*, **25**, 4, 401-409

5. El Darwish I.A., Johnston B.G., 1965, Torsion of structural shapes, *Journal of the Structural Division, ASCE*, **91**, 203-228

6. Gorzelańczyk, P., 2011, Method of fundamental solution and genetic algorithms for torsion of bars with multiply connected cross sections, *Journal of Theoretical and Applied Mechanics*, **49**, 4, 1059-1078

7. Hematiyan M.R., Doostfatemeh A., 2007, Torsion of moderately thick hollow tubes with polygonal shapes, *Mechanics Research Communications*, **34**, 7/8, 528-537

8. Hematiyan M. R., Estakhrian E., 2011, Saint-Venant torsion of open-section members of uniform thickness, *Journal of Strain Analysis for Engineering Design*, **46**, 1, 56-66

9. Lee Y.H., Sung W.J., Lee T.H., Seong K.W., 2007, Finite Element formulation of a composite double T-beam subjected to torsion, *Engineering Structures*, **29**, 2935-2945

10. Pagano, N.J., Chou, P.C., 1992, *Elasticity: Tensor, Dyadic, and Engineering Approches*, Dover Puplication 227

11. Reddy J.N., 1993, *An Introduction to the Finite Element Method*, New York: McGraw-Hill Inc.

12. Sadd M.H., 2009, *Elasticity; Theory, Application, and Numerics*, Elsevier, 2nd Edition, Academic Press

13. Timoshenko S.P., Goodier J.N., 1970, *Theory of Elasticity*, McGraw-Hill Co.

Rozwiązania w postaci zamkniętej problemu skręcania belek konstrukcyjnych z uwzględnieniem promieni przejściowych pomiędzy łączonymi segmentami

Streszczenie

W pracy przedstawiono efektywne, półanalityczne rozwiązanie problemu skręcania belek konstrukcyjnych o różnych przekrojach, takich jak T, I, H, E oraz +. Całkiem proste, a jednocześnie dokładne sformułowanie zagadnienia oparte na rozwiązaniach analitycznych i numerycznych zaprezentowano dla przypadku obliczania naprężeń ścinających w krytycznych punktach przekroju oraz wyznaczania sztywności torsyjnej elementu poddanego obciążeniu skręcającemu. Rozwiązanie zadania oparto na funkcji naprężeń Prandtla. Przekrój poprzeczny belek zdekomponowano na kilka segmentów, włączając w to elementy prostoliniowe i zakrzywione, końcowe oraz łączące. Problem skręcania rozwiązano dla każdego segmentu oddzielnie. Typowe elementy łączące przeanalizowano za pomocą metody elementów skończonych z zastosowaniem drobnej siatki. Pozostałe segmenty obliczono analitycznie. Rozwiązanie w postaci zamkniętej względem parametrów geometrycznych wyznaczono pod kątem naprężeń ścinających w krytycznych punktach każdego segmentu. Sztywność skrętną całego przekroju wyrażono również formułą w postaci zamkniętej. Zaprezentowane rozwiązania mogą być stosowane w analizie skręcania szerokiego typoszeregu od cienko- po umiarkowanie grubościennych belek konstrukcyjnych o skomplikowanym kształcie przekroju poprzecznego.

Manuscript received January 25, 2012; accepted for print July 11, 2012